

Inhibition of CaMKII α Activity Enhances Antitumor Effect of Fullerene C60 Nanocrystals by Suppression of Autophagic Degradation

Jing Xu, Hongsheng Wang, Yi Hu, Yu Shrike Zhang, Longping Wen, Fei Yin, Zhuoying Wang, Yingchao Zhang, Suoyuan Li, Yanyan Miao, Binhui Lin, Dongqing Zuo, Gangyang Wang, Min Mao, Tao Zhang, Jianxun Ding,* Yingqi Hua,* and Zhengdong Cai*


Fullerene C60 nanocrystals (nano-C60) possess various attractive bioactivities, including autophagy induction and calcium/calmodulin-dependent protein kinase II α (CaMKII α) activation. CaMKII α is a multifunctional protein kinase involved in many cellular processes including tumor progression; however, the biological effects of CaMKII α activity modulated by nano-C60 in tumors have not been reported, and the relationship between CaMKII α activity and autophagic degradation remains unclear. Herein, nano-C60 is demonstrated to elicit reactive oxygen species (ROS)-dependent cytotoxicity and persistent activation of CaMKII α in osteosarcoma (OS) cells. CaMKII α activation, in turn, produces a protective effect against cytotoxicity from nano-C60 itself. Inhibition of CaMKII α activity by either the chemical inhibitor KN-93 or CaMKII α knockdown dramatically promotes the anti-OS effect of nano-C60. Moreover, inhibition of CaMKII α activity causes lysosomal alkalization and enlargement, and impairs the degradation function of lysosomes, leading to autophagosome accumulation. Importantly, excessive autophagosome accumulation and autophagic degradation blocking are shown to play an important role in KN-93-enhanced-OS cell death. The synergistic anti-OS efficacy of KN-93 and nano-C60 is further revealed in an OS-xenografted murine model. The results demonstrate that CaMKII α inhibition, along with the suppression of autophagic degradation, presents a promising strategy for improving the antitumor efficacy of nano-C60.

Dr. J. Xu, F. Yin, Z. Wang, Dr. T. Zhang, Prof. Y. Hua, Prof. Z. Cai

Department of Orthopedics
Shanghai General Hospital
Shanghai Jiao Tong University School of Medicine
Shanghai Bone Tumor Institution
100 Haining Street, Shanghai 200080, P. R. China
E-mail: hua_yingqi@163.com; caizhengdong@sjtu.edu.cn

Dr. H. Wang, Y. Zhang, S. Li, B. Lin, Dr. D. Zuo, Dr. G. Wang, M. Mao
Shanghai Bone Tumor Institution
100 Haining Street, Shanghai 200080, P. R. China

Y. Hu
Hefei National Laboratory for Physical Sciences at the Microscale
and School of Life Sciences
University of Science and Technology of China
96 Jinzhai Street, Hefei 230026, P. R. China

 The ORCID identification number(s) for the author(s) of this article can be found under <https://doi.org/10.1002/advs.201801233>.

© 2019 The Authors. Published by WILEY-VCH Verlag GmbH & Co. KGaA, Weinheim. This is an open access article under the terms of the Creative Commons Attribution License, which permits use, distribution and reproduction in any medium, provided the original work is properly cited.

DOI: 10.1002/advs.201801233

Prof. Y. S. Zhang
Division of Engineering in Medicine
Department of Medicine
Brigham and Women's Hospital
Harvard Medical School
65 Landsdowne Street, Cambridge, MA 02139, USA

Prof. L. Wen
School of Medicine
South China University of Technology
Nanobio Laboratory
Institutes for Life Sciences
South China University of Technology
381 Wushan Street, Guangzhou 510006, P. R. China

Dr. Y. Miao
Key Laboratory of Gene Engineering of the Ministry of Education
State Key Laboratory of Biocontrol
School of Life Sciences
Sun Yat-sen University
135 West Xingang Street, Guangzhou 510275, P. R. China

Prof. J. Ding
Key Laboratory of Polymer Ecomaterials
Changchun Institute of Applied Chemistry
Chinese Academy of Sciences
5625 Renmin Street, Changchun 130022, P. R. China
E-mail: jxding@ciac.ac.cn

1. Introduction

In a wide range of nanoscale structures, inorganic nanocrystals (e.g., quantum dots, fullerene, gold, iron oxide, silica, and others) have been extensively explored as potential therapeutic systems in the field of oncology.^[1–5] Among these, fullerene C60 is of particular interest for cancer therapy due to its unique geometrical structure and remarkable physicochemical properties.^[6] The predominant use of fullerene C60 for tumor treatment has been as an antitumor reagent^[7–9] or nanocarrier.^[10,11] However, to date, our understanding regarding the antitumor biological effects that fullerenes possess remains limited.

In our previous work, we found that the water-suspended fullerene C60 nanocrystals (nano-C60) specifically bind to the hippocampal Ca²⁺ signaling protein, CaMKII α . This interaction causes persistent CaMKII α activation, as well as increased learning and memory of rats.^[12,13] CaMKII (Ca²⁺/calmodulin-dependent protein kinase II) is an important intracellular serine/threonine kinase, mainly expressed in neuronal cells. In addition to nerve signal transduction, CaMKII also plays an essential role in regulating tumor cell survival, proliferation, and differentiation.^[14–17] Nevertheless, the biological effects of nano-C60 on CaMKII α in tumors and the role of CaMKII α in the antitumor activity of nano-C60 have yet to be reported.

Several studies have documented remarkable antitumor effects of fullerenes via a variety of mechanisms involving oxidative stress,^[18] antiangiogenesis,^[19] immunomodulation,^[20] and autophagy modulation.^[21] Autophagy is a lysosomal degradation pathway in eukaryotic cells, by which unnecessary or dysfunctional cellular components are sequestered into double-membrane vesicles (autophagosomes). Then autophagosomes fuse with lysosomes to degrade and recycle the sequestered material.^[22] Autophagy has been proven to be important for intracellular quality control and cell fate-regulating processes, including cell survival during stress^[22] and cell death.^[23] As autophagy is a cellular degradation pathway, the primary physiological functions of autophagy mainly depend on its degradation capacity.^[24] For example, when cells are under stress, autophagy levels are actively elevated. This is followed by upstream autophagosome formation and downstream degradation reaching a dynamic balance state. However, if overstimulation of autophagy is maintained at a relatively high level, excessive consumption through autophagic degradation may cause cell death.^[23] Alternatively, blocking or disrupting autophagy degradation at a downstream step can lead to a large increase in the accumulation of autophagic vacuoles, which may also be catastrophic for cells.^[25,26] Therefore, modulating autophagy via autophagy induction or autophagic flux blockage has been associated with different physiological consequences, which is a promising strategy for tumor therapy.

Nano-C60 and its derivatives have been found to sensitize cancer cells to chemotherapeutic agents by inducing autophagy.^[21,27] Although these studies showed that fullerenes induce autophagosome accumulation, autophagic flux was not investigated. Moreover, the relationship between CaMKII α activity and autophagy degradation, and the influence of these two events on nano-C60-mediated cytotoxicity have not been reported.

Osteosarcoma (OS) is a primary malignant bone tumor with a high propensity of invasion and metastasis, mainly occurring in children and adolescents. Despite improvements in surgery and multi-agent chemotherapy, the 5-year survival rate of patients with OS is only approximately 65% and has remained largely unchanged over the past three decades.^[28] Several studies have proven the key role of CaMKII α in regulating OS progression and metastasis.^[29,30] Nevertheless, the underlying mechanism of CaMKII α function in OS has not been adequately clarified.

In this report, the antitumor activity of nano-C60 in OS cells with respect to CaMKII α was investigated, as illustrated in **Scheme 1**. Nano-C60 has different biological effects on OS cells, including ROS production, CaMKII α activation, and autophagy induction. First, nano-C60 elicits cytotoxicity in OS cells via ROS production. Second, nano-C60 induces abnormal autophagy, which leads to autophagosome accumulation. Third, nano-C60 causes cytoprotective autonomous CaMKII α activity against OS cell death. Pharmacological or genetic inhibition of CaMKII α enhances the anti-OS effect of nano-C60. Furthermore, this study demonstrates for the first time that CaMKII α inhibition is involved in autophagy modulation, which enhances excessive autophagosome accumulation and autophagy degradation blockage through lysosomal alkalization, enlargement, and dysfunction, and thus leads to increased nano-C60 cytotoxicity. Therefore, these results suggest that CaMKII α activity should be considered when employing nano-C60 for tumor therapy. This study provides a novel strategy for the use of CaMKII α activity and autophagic degradation as therapeutic targets to improve the efficacy of nano-C60 in tumor treatment.

2. Results

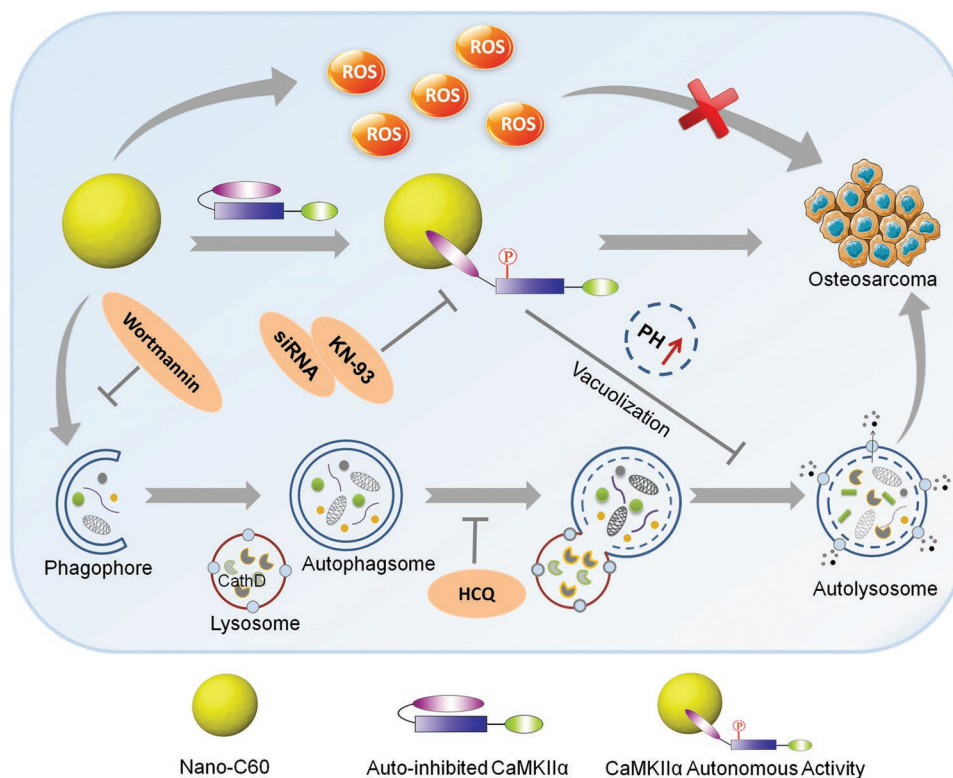
2.1. Nano-C60 Induces ROS-Dependent Cytotoxicity

Water-suspended nano-C60 was prepared using a standard tetrahydrofuran evaporation procedure,^[21] and the particles exhibited mainly circular and rectangular morphologies with an average size of 120 nm, as revealed by transmission electron microscopy (Figure S1, Supporting Information). We first evaluated the cytotoxicity of nano-C60 in a panel of OS cells (143B, MG63, Saos₂, SJSA, and HOS cells; Figure S2A, Supporting Information).

Nano-C60 is known to produce ROS.^[18,21] Consistent with this property, our preparation of nano-C60 generated ROS in 143B and MG63 cells, as detected by dihydroethidium staining (Figure S2C, Supporting Information). Reduced glutathione as a free radical scavenger could effectively reduce the cytotoxicity induced by nano-C60 (Figure S2B, Supporting Information), indicating that nano-C60 induced ROS-dependent cytotoxicity in OS cells.

2.2. Nano-C60 Elicits CaMKII α Autonomous Activity in OS Cells

Our previous report demonstrated that nano-C60-CaMKII α interaction elicits rat hippocampal CaMKII α autonomous



Scheme 1. Schematic illustration of combination treatment strategy of nano-C60 and CaMKII α inhibition for OS therapy.

activity.^[12] CaMKII is a multimeric protein usually composed of 12 subunits. Each subunit comprises three domains, an N-terminal catalytic domain for exerting catalytic function, a regulatory domain for controlling kinase activation, and a C-terminal association domain for mediating multimerization.^[31] Under resting conditions, the autoinhibitory region in the CaMKII regulatory domain interacts with the catalytic domain, which blocks the substrate binding sites and thereby inhibits CaMKII kinase activity. When intracellular Ca^{2+} levels rise, Ca^{2+} /calmodulin (Ca^{2+} /CaM) binds to the regulatory domain of CaMKII, causing the closed CaMKII conformation to open and the enzyme to become active. This activation triggers the phosphorylation of adjacent CaMKII subunits at residues T286/T287 within the autoinhibitory region, leading to Ca^{2+} /CaM-independent activity, namely, autonomous activity.^[31]

As CaMKII α is highly conserved among species, we assessed the impact of nano-C60 on CaMKII α activity in OS cells. First, we conducted in vitro assays to detect T286 phosphorylation of CaMKII α by using 143B cell lysates. Basal phosphorylation levels were very low but exhibited a 12-fold increase under Ca^{2+} /CaM treatment. This stimulated phosphorylation was significantly abolished after depleting intracellular Ca^{2+} by EGTA treatment (Figure 1A). In comparison, the addition of nano-C60 sustained the Ca^{2+} /CaM-stimulated phosphorylation even in the presence of EGTA, suggesting that nano-C60-induced phosphorylation was independent of sustained Ca^{2+} /CaM treatment. This was similar to the effect of adenosine triphosphate (ATP)-induced CaMKII α T286 autophosphorylation. Next, the nano-C60-induced T286

phosphorylation in OS cells detected by Western blot was both time (Figure 1C) and dose dependent (Figure 1B). These results indicated that nano-C60 enhanced the autonomous activity of CaMKII α in OS cells.

2.3. Inhibition of CaMKII α Activity Enhances Nano-C60-Induced Cytotoxicity

CaMKII α activation has been suggested to promote cell proliferation, invasion, and metastasis in OS.^[29,30] To evaluate the role of CaMKII α in nano-C60-induced cytotoxicity, we employed KN-93, the most extensively used inhibitor for studying in vitro and in vivo functions of CaMKII.^[32] As shown in Figure 2A, KN-93 significantly inhibited nano-C60-induced phosphorylation of CaMKII α in 143B and MG63 cells. Compared to nano-C60 treatment alone, pretreatment of cells with KN-93 further decreased 143B cell viability by approximately 25.13% (5×10^{-6} M KN-93) and 46.11% (10×10^{-6} M KN-93) (Figure 2B). Similar results were observed in MG63 cells (Figure S3, Supporting Information). The cell death rate of 143B cells detected by Hoechst 33 342/propidium iodide (PI) staining demonstrated that KN-93 enhanced nano-C60-induced 143B cell death by 30.55% (Figure 2C). These results demonstrated that combining KN-93 and nano-C60 treatments had a significant synergistic effect in OS cells.

To further confirm the role of CaMKII α in nano-C60-treated OS cells, we employed siRNA to silence CaMKII α protein expression (Figure S4, Supporting Information). Compared to the control

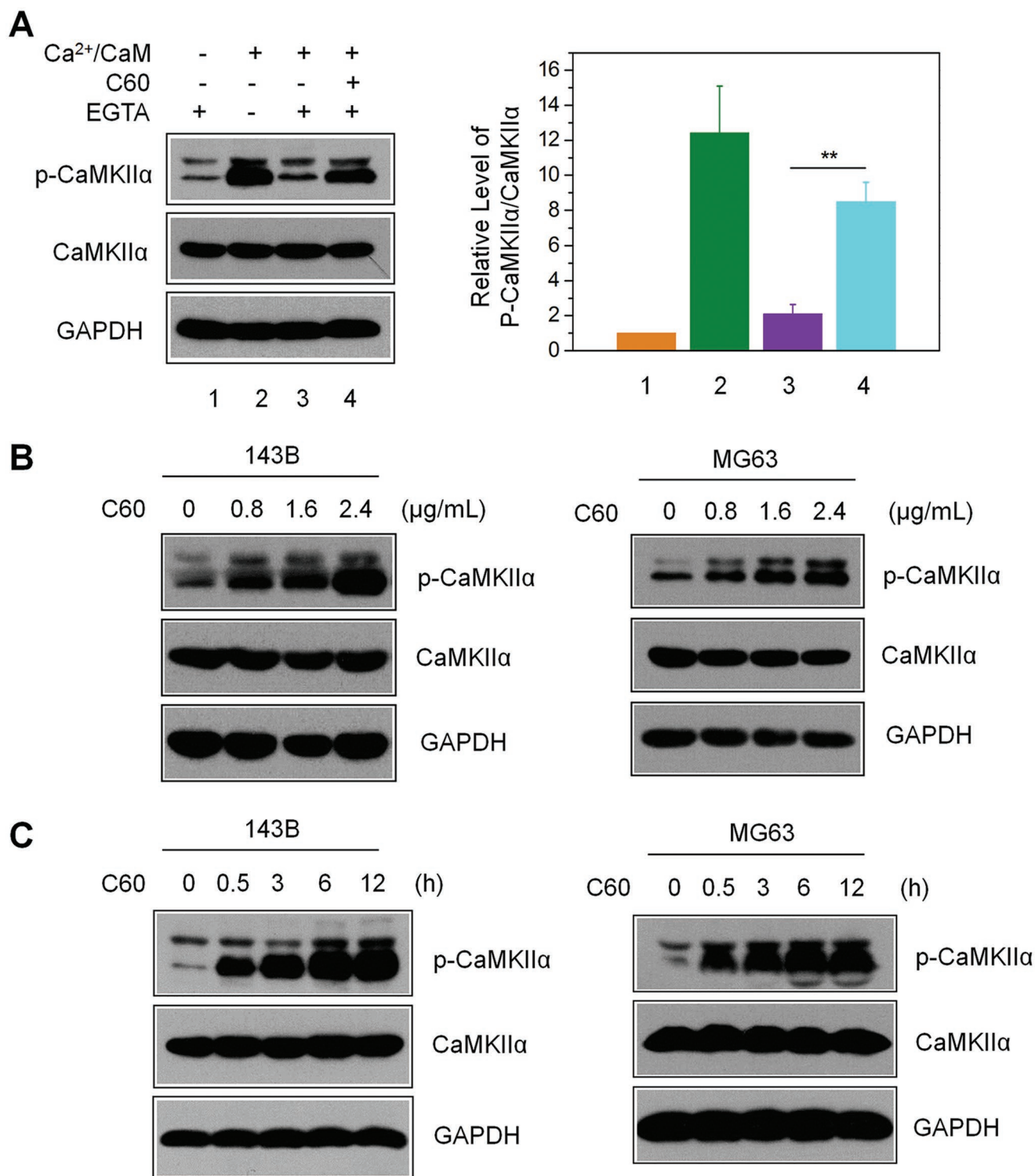


Figure 1. Nano-C60-induced autonomous CaMKII α activity in OS cells. A) T286 autophosphorylation assay for CaMKII α in 143B cell lysates, as detected by anti-CaMKII and phospho-CaMKII antibodies. The right panel shows the level of p-CaMKII α relative to total CaMKII α , with the value for control (without Ca²⁺/CaM and nano-C60) set at 1. Mean \pm SEM, $n = 3$. ** $P < 0.01$. B) Dose-dependent CaMKII α -T286 autophosphorylation level in 143B and MG63 cells treated with nano-C60 for 12 h. C) Time course of CaMKII α -T286 autophosphorylation levels in 143B and MG63 cells treated with 2.4 $\mu\text{g mL}^{-1}$ nano-C60.

siRNA group, 143B cells transfected with CaMKII α -specific siRNA followed by nano-C60 treatment exhibited a distinct decrease in cell viability (Figure 2D) and an increase in cell death (Figure 2E).

Collectively, the results above demonstrated that nano-C60-induced CaMKII α activity played a protective role in OS cell fate. Inhibition of CaMKII α activity by either the chemical

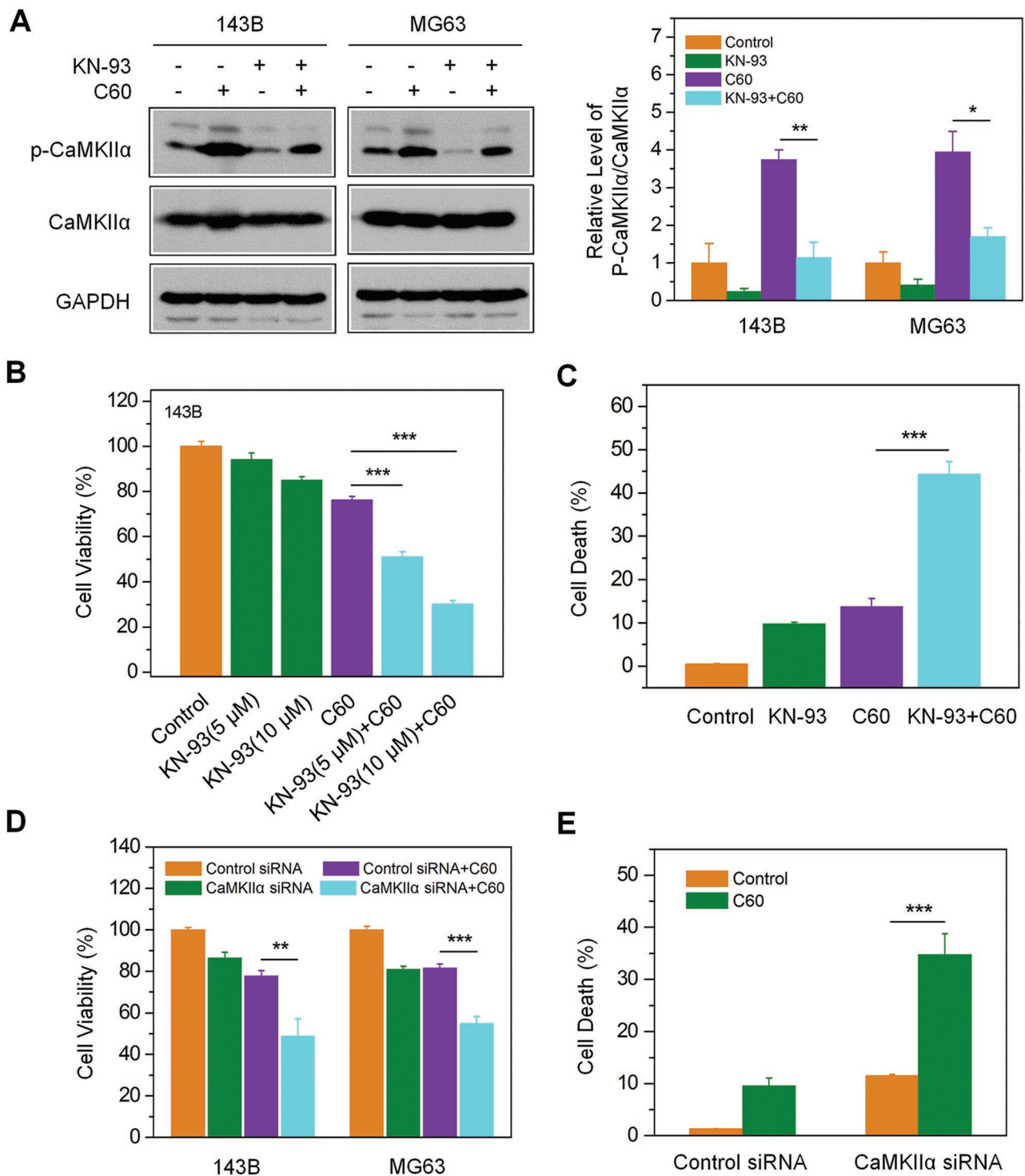


Figure 2. Effects of CaMKII α inhibition on nano-C60-induced cytotoxicity in OS cells. A) 143B and MG63 cells were treated with 1.6 $\mu\text{g mL}^{-1}$ of nano-C60 in the presence or absence of 10.0×10^{-6} M KN-93 for 24 h. CaMKII α level was detected by Western blotting with antibodies against CaMKII and phospho-CaMKII. The right panel demonstrates the level of p-CaMKII α relative to that of total CaMKII α , with the control value (without nano-C60) set at 1. Mean \pm SEM, $n = 3$. * $P < 0.05$, ** $P < 0.01$. B) 143B cells were treated with or without 1.6 $\mu\text{g mL}^{-1}$ of nano-C60 in the presence or absence of 5.0 or 10.0 $\times 10^{-6}$ M KN-93 for 24 h. Cell viability was measured by CCK-8 assay. Mean \pm SEM, $n = 3$. *** $P < 0.005$. C) Cell death assay of 143B cells treated as in A). Cell death rates were determined by Hoechst/PI staining and demonstrated as the percentage of PI-positive cells. Mean \pm SEM, $n = 3$. *** $P < 0.005$. D) Cell viability of 143B and MG63 cells treated with or without 1.6 $\mu\text{g mL}^{-1}$ of nano-C60 for 24 h after transfection with CaMKII α siRNA or control siRNA for 48 h. Mean \pm SEM, $n = 3$. ** $P < 0.01$, *** $P < 0.005$. E) The cell death rates of 143B cells treated as described in D). Mean \pm SEM, $n = 3$. *** $P < 0.005$.

inhibitor KN-93 or by CaMKII α knockdown enhanced the cytotoxicity of nano-C60 in OS cells.

2.4. Inhibition of CaMKII α Activity Promotes Nano-C60-Induced Autophagosome Accumulation and Impairs Autophagic Degradation

A previous report revealed that nano-C60 induces autophagy and sensitizes cancer cells to chemotherapeutic killing,^[21] which inspired us to investigate the potential relationship between nano-C60-stimulated autophagy and CaMKII α activity. As the conversion from soluble microtubule-associated protein 1 light chain 3 (LC3-I) to insoluble LC3 (LC3-II) is a hallmark of autophagy,^[33] we used MG63 cells expressing enhanced green fluorescent protein-tagged LC3 (MG63-EGFP-LC3) to assess the autophagy-inducing ability of nano-C60 in OS. The green fluorescence of EGFP-LC3 was diffuse throughout the cytoplasm of control cells, while several bright green punctate structures accumulated in the nano-C60-treated cells (Figure 3C). Moreover, the level of LC3-II was significantly elevated in a dose-dependent manner after nano-C60 treatment, as shown by Western blot analysis (Figure 3A). These data suggested that nano-C60 caused the accumulation of autophagosomes in OS cells.

As autophagy is a dynamic process, autophagosome accumulation may be due to the increase in autophagosome formation (autophagy induction) or the decrease in autophagosome degradation.^[34] To detect the autophagic flux induced by nano-C60, we treated cells with hydroxychloroquine (HCQ), a classic autophagy inhibitor that disrupts autolysosome degradation by blocking vacuolar H⁺-ATPase activity. The addition of HCQ significantly enhanced nano-C60-induced LC3-II accumulation in both 143B and MG63 cells, indicating that nano-C60 enhanced new autophagosome formation (Figure 3B). SQSTM1/P62, an LC3-binding protein, is degraded via autophagy.^[35] Interestingly, the abundance of SQSTM1/P62 increased after nano-C60 treatment (Figure 3A), and co-treatment with HCQ and nano-C60 further increased the level of SQSTM1/P62 (Figure 3B), which indicated a possible impairment of nano-C60-induced autophagy turnover.

Next, we examined the impact of CaMKII α inhibition on nano-C60-induced autophagy. As shown in Figure 3C, KN-93 markedly enhanced the formation of green punctate dots in nano-C60-treated cells, and Western blotting results showed an increased accumulation of LC3-II (Figure 3D), but a decreased degradation of SQSTM1/P62 in these cells (Figure 3E). These results suggested that inhibition of CaMKII α activity promoted nano-C60-induced autophagosome accumulation and reduced autophagic degradation in OS cells.

2.5. Nano-C60 and KN-93 Co-Treatment Causes Lysosomal Alkalinization and Enlargement

Several types of inorganic nanoparticles, including gold nanoparticles^[36] and surface-functionalized silica nanoparticles,^[37] have been reported to cause lysosomal dysfunction. As autophagy is a kind of lysosome-based degradative pathway, disruption of lysosomal function or impairment of the lysosomal degradation capacity may block autophagic flux. Lysosomal-associated membrane protein 1 (Lamp-1) is a classic marker for lysosomal membranes. Confocal imaging of red fluorescence protein

(RFP)-Lamp-1 in 143B cells revealed that nano-C60 and KN-93 co-treatment promotes lysosomal enlargement and vacuolization (Figure 4A), which likely represent a state of profound lysosomal stress and dysfunction.^[38,39] It is well documented that defective lysosomal degradation induces lysosomal enlargement.^[40] The normal lysosomal degradation function depends on an acidic environment, and thus, we measured the acidity of lysosomes in 143B-RFP-Lamp1 cells with LysoSensor Green DND-189, which is an acidotropic dye exhibiting the increase in the fluorescence intensity under acidification.^[41] To attenuate the influence of significant cytotoxicity induced by the combination treatment on lysosomal acidity, we used a relatively low dose (1.0 $\mu\text{g mL}^{-1}$ of nano-C60 and 7.5×10^{-6} M KN-93 for 12 h). Fluorescence imaging (Figure 4B) and flow cytometric analysis (Figure 4C) showed that the fluorescence intensity of LysoSensor Green was slightly reduced in KN-93-treated cells but was dramatically reduced in cells co-treated with KN-93 and nano-C60. Furthermore, LysoSensor Green was well colocalized with RFP-Lamp1, which confirmed that the acidic compartments stained by LysoSensor Green were Lamp1 positive structures (lysosomes) (Figure 4B). These data indicated that the combination treatment caused alkalinization and enlargement of lysosomes.

2.6. Nano-C60 and KN-93 Co-Treatment Impairs the Lysosomal Degradation Capacity

To determine whether the combination treatment impairs the lysosomal degradation capacity, we pretreated MG63-EGFP-LC3 cells with a lysosomal degradation indicator, derivative-quenched bovine serum albumin (DQ-BSA).^[42] Enzymatic cleavage of DQ-BSA in lysosomes results in the generation of fluorescent fragments. A large number of red fluorescent fragments (dequenching of DQ-BSA) occurred in the control group. In contrast, very a few red fluorescent fragments occurred in the co-treatment group (Figure 5A), indicative of the impairment of lysosomal degradation capacity. Moreover, the dequenching of DQ-BSA was negatively correlated with GFP-LC3B puncta (Figure 5A), suggesting that the inhibition of lysosomal degradation resulted in the accumulation of autophagosomes.

Cathepsins (cathepsin B and cathepsin D), the classical lysosomal marker proteases, participate in autophagic degradation.^[43] Then, we detected the effect of the combination treatment on the lysosomal proteolytic activity. As shown in Figure 5B,C, the maturation levels of cathepsin B and cathepsin D in 143B and MG63 cells were dramatically reduced after co-treatment.

Taken together, we speculated that nano-C60 and KN-93 co-treatment promoted lysosomal alkalinization and impaired the lysosomal degradation capacity, leading to inhibition of autophagic degradation and autophagosome accumulation, and thus causing lysosomal vacuolization and enlargement.

2.7. Excessive Autophagosome Accumulation Contributes to the Cytotoxicity Elicited by Nano-C60 and KN-93 Combination Treatment

To evaluate the role of autophagic degradation in the cytotoxicity elicited by nano-C60 and KN-93 co-treatment, we employed an upstream autophagy inhibitor, wortmannin

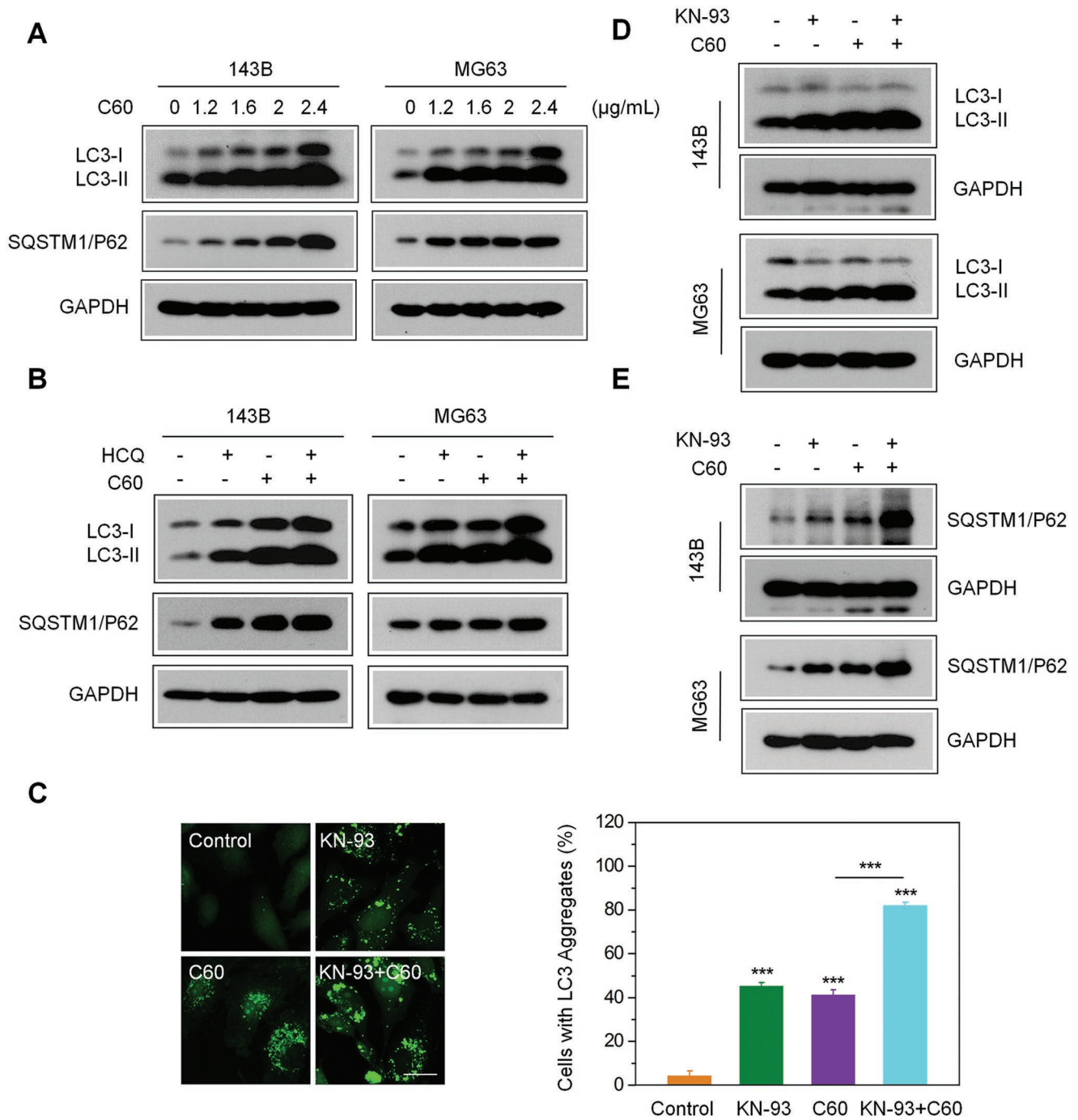


Figure 3. Enhancement of nano-C60-induced incomplete autophagy by CaMKII α inhibition. A) Western blotting for the expression of autophagy-associated proteins in 143B and MG63 cells treated with different doses of nano-C60 for 24 h using antibodies against LC3, SQSTM1/P62, and GAPDH. B) 143B cells were treated with or without 1.6 $\mu\text{g mL}^{-1}$ nano-C60 in the presence or absence of 100.0×10^{-6} M HCQ for 24 h. LC3 and SQSTM1/P62 levels were examined by Western blotting with anti-LC3 and anti-SQSTM1/P62 antibodies, respectively. C) Representative fluorescence microscopy images of MG63-EGFP-LC3 cells treated with or without 1.6 $\mu\text{g mL}^{-1}$ of nano-C60 in the presence or absence of 10.0×10^{-6} M KN-93 for 24 h. Scale bar = 20.0×10^{-6} m. The right panel demonstrates the rate of EGFP-LC3 dots-positive cells. Mean \pm SEM, $n = 3$. *** $P < 0.005$. D,E) Western blot analysis of the expression of LC3-II and SQSTM1/P62 in 143B and MG63 cells treated with or without 1.6 $\mu\text{g mL}^{-1}$ of nano-C60 in the presence or absence of 10.0×10^{-6} M KN-93 for 24 h.

(Wort), and a downstream autophagy inhibitor, HCQ. The addition of HCQ after nano-C60 and KN-93 co-treatment dramatically increased LC3-II and SQSTM1/P62 accumulation

(Figure 6A), decreased cell viability (Figure 6B), and enhanced cell death (Figure 6E). These results indicated that the accumulation of autophagosomes and the inhibition of autophagic

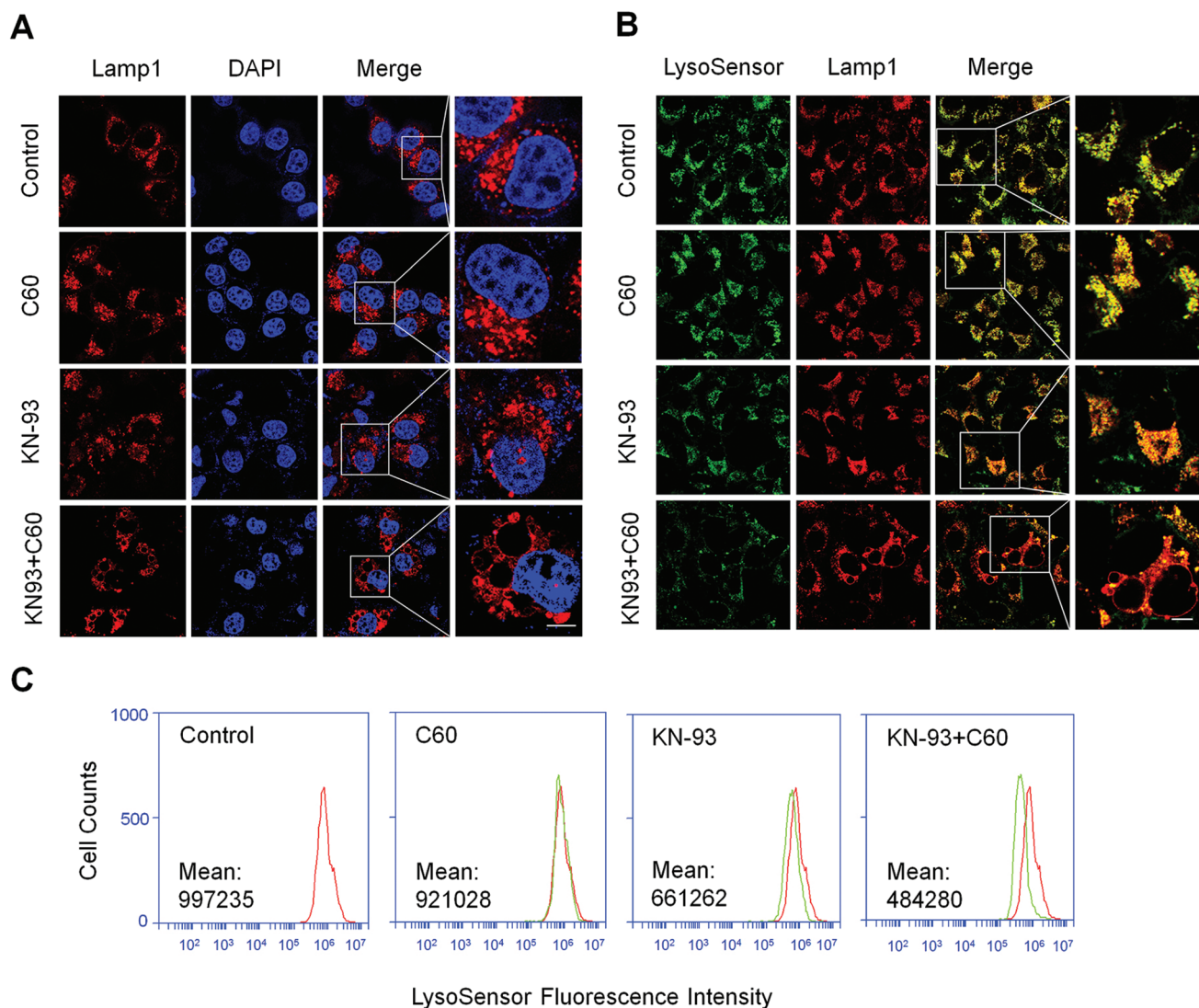


Figure 4. Lysosomal alkalinization and enlargement caused by nano-C60 and KN-93 combination treatment. A) Representative fluorescence images of 143B-RFP-Lamp1 cells treated with or without $1.6 \mu\text{g mL}^{-1}$ of nano-C60 in the presence or absence of $10.0 \times 10^{-6} \text{ M}$ KN-93 for 16 h. Nuclei were stained with DAPI (blue). Scale bar = $20.0 \mu\text{m}$. B) Representative fluorescence images of lysosome acidity using LysoSensor Green DND-189 staining in 143B-RFP-Lamp1 cells treated with or without $1.0 \mu\text{g mL}^{-1}$ of nano-C60 in the presence or absence of $7.5 \times 10^{-6} \text{ M}$ KN-93 for 12 h. Scale bar = $50.0 \mu\text{m}$. C) Flow cytometric analysis of lysosome acidity in 143B cells treated as described in B).

degradation further enhanced the cytotoxicity elicited by the combination treatment.

Next, we alleviated autophagosome accumulation through an upstream autophagy inhibitor Wort, which blocks autophagosome formation via suppression of the class III phosphatidylinositol 3-kinase (PtdIns3K) signaling pathway. Wort effectively inhibited LC3-II conversion induced by nano-C60 alone (Figure S5A, Supporting Information) or nano-C60 and KN-93 co-treatment (Figure 6C), and decreased the cytotoxicity of nano-C60 itself (Figure S5B, Supporting Information). Furthermore, pretreatment with Wort promoted cell viability (Figure 6D) and attenuated cell death (Figure 6E) after nano-C60 and KN-93 co-treatment.

From these results, we concluded that autophagic degradation is involved in the nano-C60 and KN-93 combined

treatment-induced biological effects in OS cells. KN-93 enhanced nano-C60-elicited cytotoxicity through autophagic degradation inhibition and the excessive autophagosome accumulation.

2.8. Inhibition of CaMKII α Activity Enhances the Anti-OS Efficacy of Nano-C60 In Vivo

To determine the synergistic ablation effect of nano-C60 and KN-93 in vivo, a 143B-derived subcutaneous tumor xenograft model was established. BALB/c nude mice were injected with 143B cells in the right armpit. On the 8th day postinjection, tumor-bearing mice were randomly divided into four groups: PBS (control), KN-93, nano-C60, and KN-93+nano-C60. Mice

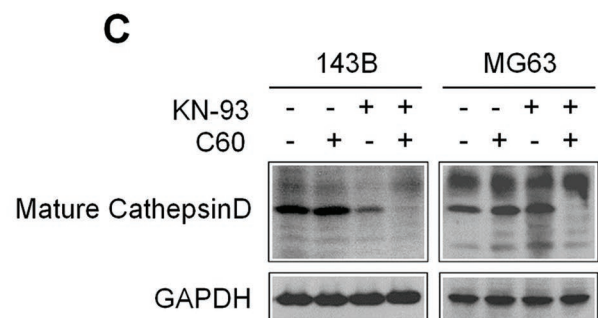
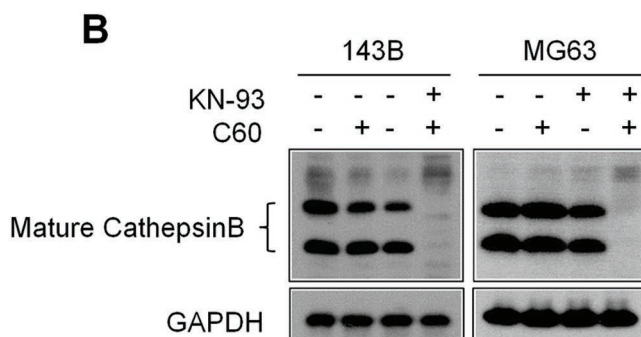
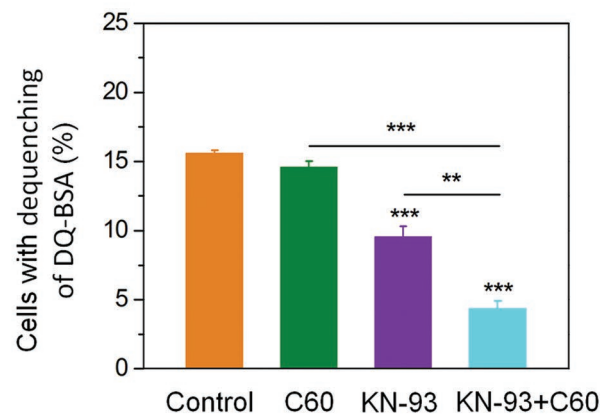
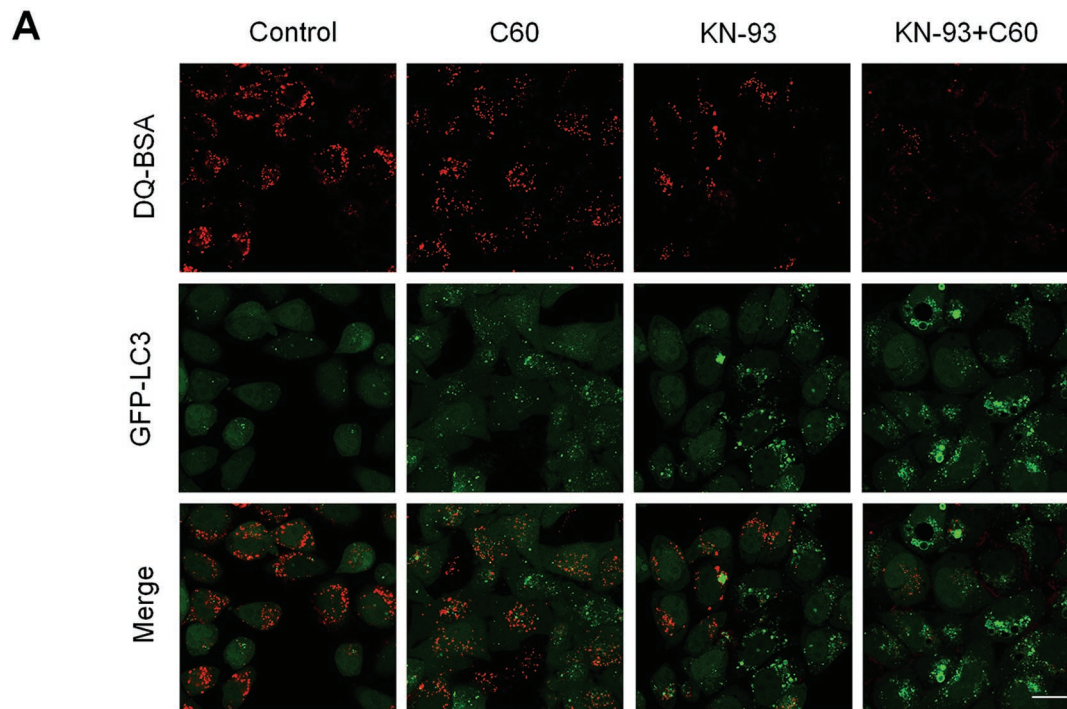


Figure 5. Impaired lysosomal degradation capacity caused by nano-C60 and KN-93 combination treatment. A) DQ-BSA analysis of lysosomal proteolytic activity in 143B cells treated with or without $1.0 \mu\text{g mL}^{-1}$ of nano-C60 in the presence or absence of $7.5 \times 10^{-6} \text{ M}$ KN-93 for 12 h. The average number of the red fluorescent fragments in each cell was quantified (lower panel). At least 60 cells were analyzed for each treatment. Mean \pm SEM, $n = 3$. $**P < 0.01$ $***P < 0.005$. Scale bar = $50.0 \mu\text{m}$. B) and C) Western blot analysis of enzymatic activity of cathepsin B and cathepsin D in 143B and MG63 cells treated with or without $1.6 \mu\text{g mL}^{-1}$ of nano-C60 in the presence or absence of $10.0 \times 10^{-6} \text{ M}$ KN-93 for 24 h.

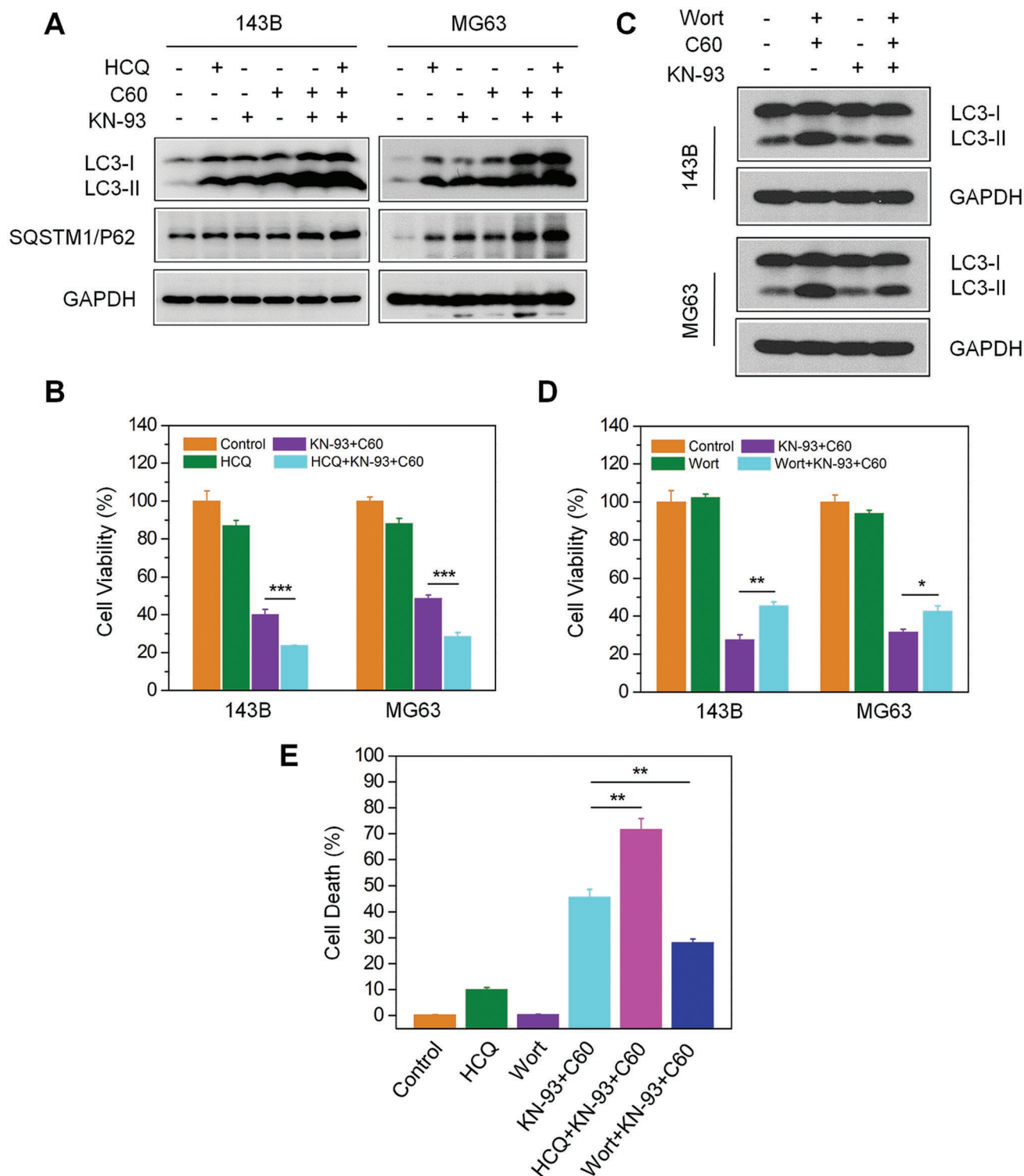


Figure 6. Effects of autophagosome accumulation on cytotoxicity induced by nano-C60 and KN-93 combination treatment. A,B) Before $1.6 \mu\text{g mL}^{-1}$ of nano-C60 and $10.0 \times 10^{-6} \text{ M}$ KN-93 addition, 143B cells were pretreated with or without $100.0 \times 10^{-6} \text{ M}$ HCQ. A) LC3 and SQATM1/P62 levels were detected by Western blotting using anti-LC3 and anti-SQATM1/P62 antibodies, respectively, and B) cell viability was assessed by CCK-8 assay. Mean \pm SEM, $n = 3$. $***P < 0.005$. C) Before $1.6 \mu\text{g mL}^{-1}$ of nano-C60 and $10 \times 10^{-6} \text{ M}$ KN-93 addition, 143B and MG63 cells were pretreated with or without $100.0 \times 10^{-9} \text{ M}$ Wort. LC3 levels were detected by Western blotting using anti-LC3 and anti-SQATM1/P62 antibodies, respectively. D) Cell viability of each group treated as described in C) was assessed by CCK-8 assay. Mean \pm SEM, $n = 3$. $*P < 0.05$, $***P < 0.01$. E) Before nano-C60 and KN-93 addition, 143B cells were pretreated with or without HCQ or Wort. Cell death assay was determined by Hoechst/PI staining and demonstrated as the percentage of PI-positive cells. Mean \pm SEM, $n = 3$. $**P < 0.01$. Scale bar = $200.0 \mu\text{m}$.

were administered a dose every other day, and tumor size and body weight were also measured. After two weeks of treatment, the mice were sacrificed, and their subcutaneous tumors were gently removed, photographed, and weighed. No significant changes in body weight were observed after any of the treatments (Figure S6, Supporting Information). As depicted in **Figure 7A,B**, tumor volume results indicated that nano-C60 alone and KN-93 alone slightly inhibited tumor growth. However, in comparison to the single-drug treatments, the combination of KN-93 and nano-C60 significantly suppressed tumor growth. Similar results were observed in tumor weight (Figure 7C). These results confirmed that combined treatment of nano-C60 with KN-93 had a significant synergistic effect in ablating OS.

Furthermore, terminal deoxyribonucleotidyl transferase (TDT)-mediated dUTP-digoxigenin nick end labeling (TUNEL) staining demonstrated that there were more apoptotic cells in the tumors of the co-treatment group than in those of the single-drug groups (Figure 7D), which was consistent with results from hematoxylin and eosin staining (Figure S7, Supporting Information). In addition, immunoblot analysis of the tumor tissues demonstrated that the expression of phosphorylated CaMKII α was effectively inhibited, while the level of autophagy was significantly elevated after the combination treatment (Figure 7E). Collectively, the results above show that inhibition of CaMKII α activity enhances the antitumor efficacy of nano-C60 in OS.

3. Discussion

In this report, we demonstrated that nano-C60 elicited ROS-dependent anti-OS activity. Moreover, the autonomous CaMKII α activity induced by nano-C60 played a protective role in OS cell fate and attenuated the anticancer effect of nano-C60. KN-93, the most widely used CaMKII inhibitor, has been found to cause cell cycle arrest or cell death in a variety of tumors.^[44] Few studies have reported the combination treatment of KN-93 and anticancer agents, especially nanodrugs. In this study, we showed that in comparison to a single-agent treatment at the same concentration, the combination of KN-93 and nano-C60 at a relatively low dose exerted outstanding synergistic anti-OS effects *in vitro* and *in vivo*. These results supported the potential use of KN-93 in adjunct with nano-C60 for OS therapy. Considering that CaMKII α is important for tumor progression in several tumor types,^[14–17] we speculate that CaMKII α inhibition may improve the efficacy of nano-C60 in other tumors with high expression of CaMKII α as well. Further studies are required to address these possibilities.

Under normal physiological conditions, autophagy occurs at a relatively low basal level, playing a cytoprotective role by maintaining cellular homeostasis. During tumor development, elevated levels of autophagy play paradoxical roles in promoting both cell survival and cell death.^[45] Recent studies demonstrated that fullerene C60 and its derivatives act as autophagy activators that sensitize cancer cells to chemotherapeutic killing.^[21,27] Nevertheless, in these studies, only autophagosome accumulation was shown, with no autophagic flux investigated. In the current work, we examined the autophagic response elicited by nano-C60 in detail and discovered that nano-C60 induced

an increase in autophagosome formation and a decrease in autophagic turnover.

Interestingly, inhibition of CaMKII α further promoted nano-C60-induced autophagy. Currently, only a few groups have shown the involvement of CaMKII in autophagy initiation. For example, inhibition of CaMKII γ has been shown to trigger apoptosis and autophagy in colorectal cancer cells.^[46] Nevertheless, the detailed influence of CaMKII on autophagic degradation has not been reported. Herein, we further demonstrated that inhibition of CaMKII by KN-93 in nano-C60-treated cells enhanced autophagosome and SQSTM1/P62 accumulation, suggesting the ability of KN-93 to promote incomplete autophagy induced by nano-C60. Unexpectedly, Zhong et al. showed that activation of CaMKII was required to initiate autophagy in response to free fatty acids, and this activation was significantly inhibited by KN-93 in a cardiac remodeling model.^[47] In human muscle cells, CaMKII inactivation by obestatin signaling contributed to the inhibition of FoxO-dependent autophagy.^[48] In these findings, the relationship between CaMKII and autophagy conflicted with our current study. It is conceivable that CaMKII has diverse effects on autophagy by sensing various upstream signals and acting on distinct downstream targets in different cells and conditions.

Lysosomes, as the major intracellular degradation organelle, play an essential role in the degradation of aggregated or malfunctioning proteins (e.g., via autophagy).^[49] Thus, lysosomal dysfunction has serious physiological and pathological consequences.^[40] In this study, we found for the first time that inhibition of CaMKII promoted lysosomal alkalization, enlargement, and vacuolization, whereas nano-C60 had no significant effect on lysosomal acidity. It is well documented that defective lysosomal degradation can induce lysosomal enlargement.^[40] Therefore, we speculate that KN-93 disrupts the lysosomal degradation capacity by altering the acidic environment, thus enhancing nano-C60-induced autophagic flux inhibition. Moreover, blocking autophagic degradation further increases lysosomal enlargement and vacuolization. Thus, it is reasonable to speculate that the biological effects of KN-93 and nano-C60 on lysosomes reciprocally influence each other. Combining KN-93 with nano-C60 synergistically enhances lysosomal dysfunction and autophagic turnover inhibition. Nevertheless, the exact molecular mechanism of KN-93 action on lysosomes remains undetermined.

One intriguing finding in the present study is that the downstream autophagy inhibitor HCQ enhanced the cytotoxicity induced by nano-C60 and KN-93 combination treatment, while the upstream autophagy inhibitor Wort had the opposite effect. These results indicated a correlation between excessive autophagosome accumulation and cell death. Since autophagy is now under investigation to enhance the efficacy of antitumor therapy, it is important to notice the different role of autophagy in tumor therapy. Our data provided a model that precise control of autophagy could maximize the antitumor effect of nanomaterials.

Phosphatidylinositol 3-kinases (PtdIns3Ks) and phosphoinositide 3-kinases (PI3Ks) are all involved in the autophagic process. As we all know, Wort blocks autophagosome formation via suppression of the class III PtdIns3K pathway, which is a positive regulator of autophagy.^[50] However, PI3-Kinases have their ATP binding sites at the kinase domain in common since they are evolutionarily related. Therefore, Wort was also found to interfere with the activity of class I PI3-Kinase by blocking the

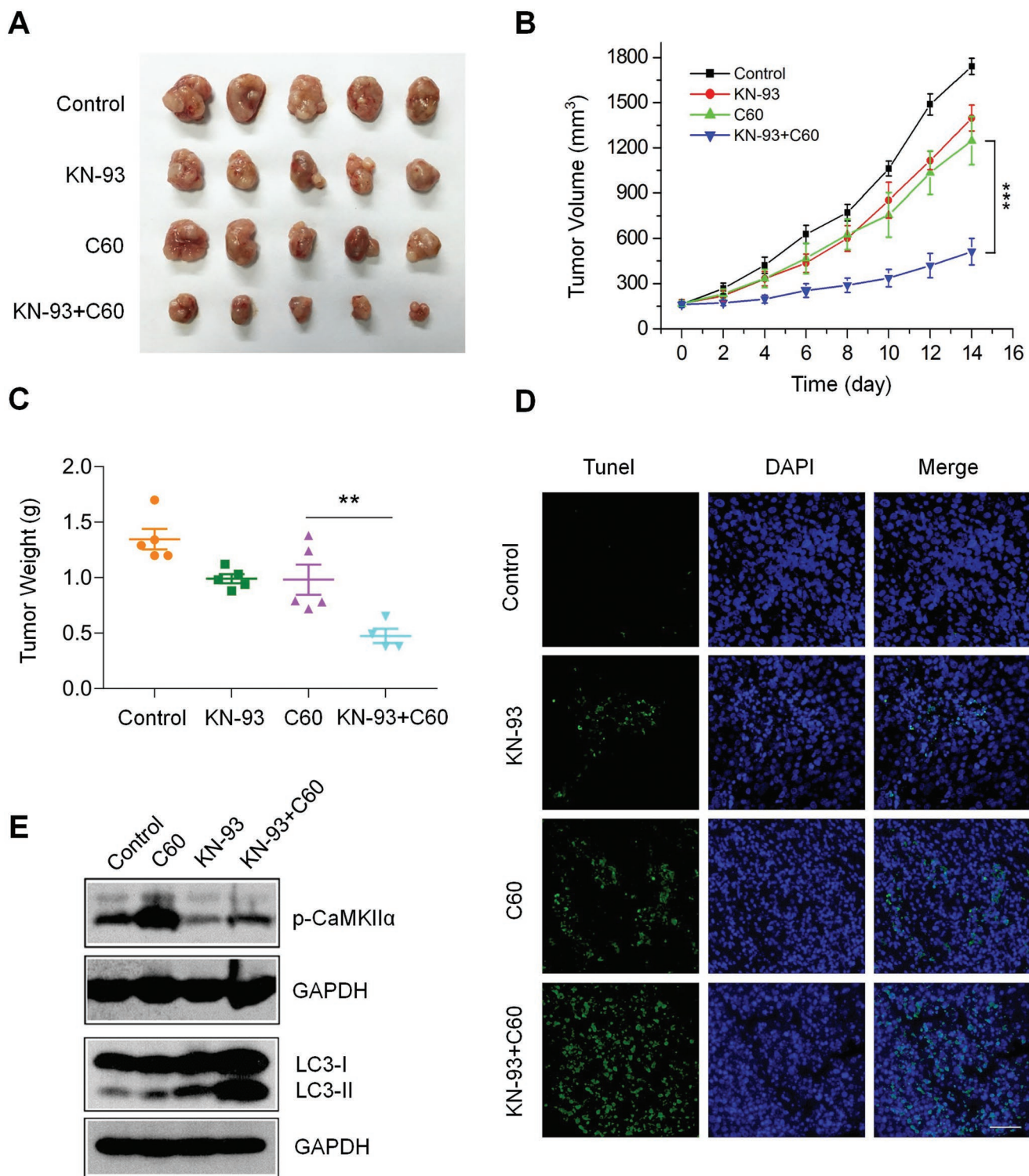


Figure 7. Enhanced synergistic anti-OS efficacy of nano-C60 by CaMKII α inhibitor KN-93 in vivo. A) Tumors from nude mice treated with PBS (control), 0.5 mg kg^{-1} KN-93 (s.c.), 0.2 mg kg^{-1} nano-C60 (s.c.), or 0.5 mg kg^{-1} KN-93 plus 0.2 mg kg^{-1} nano-C60 (s.c.). B) Tumor volume and C) tumor weight in each group are shown. Mean \pm SEM, $n = 5$. $**P < 0.01$, $***P < 0.005$. D) TUNEL staining (green) of tumor tissues was performed to detect apoptotic cells, and nuclei were treated with DAPI (blue). Scale bar = $50.0 \mu\text{m}$. E) Western blot analysis of the levels of phospho- or total-CaMKII α , and LC3 in tumor tissues.

ATP binding site. Class I PI3-Kinase inhibits autophagy through the well-documented PI3K-AKT-mTOR complex 1 (MTORC1) pathway and involves in cell survival, metabolism, migration,

etc.^[50] Thus, Wort inhibits autophagy only in a certain “pharmacological window.” In our study, Wort effectively inhibited LC3-II conversion induced by nano-C60 alone (Figure S5A,

Supporting Information) or nano-C60 and KN-93 co-treatment (Figure 6C); nevertheless, there was no obvious effect on the class I PI3K-AKT signaling (Figure S8, Supporting Information). These results eliminated the interference of Wort on class I PI3K-AKT signaling and demonstrated that Wort at the concentration we used was able to inhibit autophagy.

Another interesting point is that nano-C60 requires photoactivation for ROS production.^[18,21] This requirement appears to be minimal, as normal laboratory light exposure during cell handling was sufficient to induce ROS production. Nonetheless, as minimal light exposure cannot be achieved in most in vivo conditions, the cytotoxicity induced by nano-C60 alone may be weaker in vivo than in vitro. Therefore, in addition to photoactivation, the antitumor effect of nano-C60 should be improved through other methods such as drug combination.

Collectively, this report demonstrates the antagonism of nano-C60-CaMKII α interactions in nano-C60-induced antitumor effect. CaMKII α inhibition sensitizes OS cells to nano-C60 through suppression of autophagic degradation. So, these findings suggest that CaMKII α activity should be considered when employing nano-C60 for tumor therapy. Therefore, our study provides new guidance for the rational design and synthesis of nano-C60-based antitumor nanomedicines. For instance, a new nanoplatform based on nano-C60 can be designed to combine CaMKII α inhibition, autophagy modulation, with other strategies such as photodynamic therapy for augmenting nano-C60-elicited antitumor capacity.

4. Conclusion

In summary, we confirmed the biological effect of nano-C60–CaMKII α interactions on tumor therapy and investigated the relationship between CaMKII α inhibition and autophagic degradation. In addition to its direct cytotoxic effect via ROS production, nano-C60 was found to have a strong ability to induce autonomous CaMKII α activity in OS cells. Nevertheless, CaMKII α activation played a cytoprotective role to counteract nano-C60-induced cytotoxicity. Inhibition of CaMKII α activity by either the chemical inhibitor KN-93 or CaMKII α knockdown significantly enhanced the antitumor effect of nano-C60 in vitro and in vivo. Mechanistically, CaMKII α inhibition caused lysosomal dysfunction through lysosomal alkalization, which inhibited autophagic degradation and promoted abnormal autophagosome accumulation, leading to an increase in nano-C60-induced cytotoxicity in OS cells. Importantly, the downstream autophagy inhibitor HCQ enhanced cell death after nano-C60 and KN-93 co-treatment, whereas the upstream autophagy inhibitor Wort has the opposite effect. These results indicated that excessive autophagosome accumulation and autophagic degradation blocking play an important role in KN-93-enhanced-OS cell death. This data provides a model demonstrating that precise control of autophagy maximizes the antitumor effect of nanomaterials. Therefore, inhibiting CaMKII α activity renders OS cells more vulnerable to nano-C60 by suppressing autophagic degradation, which may represent a novel and effective strategy for improving the efficacy of nano-C60 in antitumor therapy.

5. Experimental Section

Materials: Ultrapure water (pH 6.7; Milli-Q, Bedford, MA, USA) was used for all experimental conditions. Fullerene C60 (99.9% pure) and KN-93 (Cat. No. K1385) were purchased from Sigma-Aldrich. Bovine CaM (Cat. No. 208 690) was purchased from Calbiochem. Wort (Cat. No. S2758) and HCQ (Cat. No. S4430) were purchased from Selleckchem. Antibodies against CaMKII (Cat. No. ab52476) and phospho-T286 CaMKII (Cat. No. ab32678) were purchased from Abcam. Anti-LC3 antibody (NB100-2220) was purchased from Novus Biologicals. Antibodies against SQSTM1/p62 (39749), phospho-AKT (4060), total AKT (4691), cathepsin B (31718), cathepsin D (2284) were purchased from Cell Signaling Technology. Anti-GAPDH antibody (Cat. No. MAB374) was purchased from Millipore. Alexa Fluor 594 AffiniPure Goat anti-rabbit IgG was purchased from Jackson ImmunoResearch Laboratories.

CaMKII α Autophosphorylation: Briefly, 143B cell lysates were pretreated with 500.0×10^{-6} M CaCl₂, 1.0×10^{-6} M CaM, and 10.0×10^{-3} M MgCl₂ for 1 min on ice, and $4.0 \mu\text{g mL}^{-1}$ of nano-C60 was subsequently added and then incubated for 20 min, followed by the addition of 1.0×10^{-3} M EGTA for another 10 min on ice. CaMKII α phosphorylation was triggered by treatment with 1.0×10^{-3} M ATP and terminated with sodium dodecyl sulfate (SDS) loading buffer after 30 min. CaMKII α autophosphorylation at residue T286 was measured by Western blotting with the anti-phospho-CaMKII antibody.

Cell Death Assay: Cells were treated with 10.0×10^{-3} M Hoechst 33342 and 10.0×10^{-3} M PI for 20 min. After washing with PBS three times, cells were detected by fluorescence microscopy (Leica, Wetzlar, Germany). Cell death was quantified by counting at least 400 cells per group and was expressed as the ratio of PI-positive to Hoechst 33 342-positive cells. These assays were independently completed by two of the authors in a double-blind manner.

CaMKII α siRNA Transfection: For siRNA transfection, 143B cells were cultured in 6-well plates. After 12 h, the cells were transfected with 20.0×10^{-9} M of CaMKII α siRNA (sc-29 900, Santa Cruz Biotechnology, Santa Cruz, CA, USA) per well using Lipofectamine 2000 (Invitrogen, USA) and following the manufacturer's protocol.

EGFP-LC3 Puncta Formation Assay: EGFP-LC3 puncta was quantified by counting at least 200 cells and demonstrated as the percentage of EGFP-LC3-positive cells (cells with at least five EGFP-LC3 dots). The assays were independently completed in a double-blind manner.

Lysosomal Acidity Assay: 143B cells were treated with $1.0 \mu\text{g mL}^{-1}$ nano-C60 in the presence or absence of 7.5×10^{-6} M KN-93 for 12 h and were then harvested and washed twice in PBS. After incubating with $500.0 \mu\text{L}$ of prewarmed medium containing 1.0×10^{-6} M LysoSensor Green DND-189 dye (L-7535, Invitrogen, USA) for 30 min, cells were washed and resuspended with PBS. Lysosomal acidity was analyzed by flow cytometry (FACSCalibur, BD, San Jose, CA, USA).

DQ-BSA Assay: MG63-EGFP-LC3 cells were incubated in DMEM containing DQ Red BSA (D-12051, Molecular Probes) at a final concentration of $10.0 \mu\text{g mL}^{-1}$ for 3 h at 37 °C, washed twice with PBS and imaged by fluorescence microscopy (Leica, Wetzlar, Germany). The number of the fluorescent fragments in each cell was quantified, and at least 60 cells were included for each group.

Animals and Tumor Models: Male BALB/c nude mice (6–8 weeks) were purchased from Shanghai Slac Laboratory Animal Co., Ltd. (Shanghai, China). Next, 143B tumor cells (1.0×10^6) resuspended in $100.0 \mu\text{L}$ of cold PBS were inoculated into the right flank of each nude mouse. After 1 week, mice were randomly divided into four groups (five mice in each group): PBS, nano-C60 alone, KN-93 alone, and nano-C60+KN-93. Nano-C60 ($0.2 \text{ mg kg BW}^{-1}$) and KN-93 ($0.5 \text{ mg kg BW}^{-1}$) were subcutaneously (s.c.) injected into the tumor every 2 days. Body weight and tumor sizes were also measured every 2 days. Tumor volume was estimated using the following equation:

$$\text{Tumor Volume} = \frac{\text{Length} \times \text{Width}^2}{2}$$

After 14 days, all mice were sacrificed, and tumors were removed and weighed. All animal care and experimental procedures were approved by the Animal Care and Use Committee of Shanghai General Hospital.

TUNEL Assay: Apoptosis was detected using an In Situ Cell Death Detection Kit, Fluorescein (Roche Diagnostics, Mannheim, Germany). Paraffin-embedded 143B tumor sections were deparaffinized using xylene and ethanol. Then, the sections were rehydrated by addition of proteinase K at room temperature for 3 min and incubation with equilibration buffer for 30 min. The TUNEL reaction mixture was added to the sections and then incubated at 37 °C for another 60 min. After washing twice with PBS, the sections were stained with DAPI, and randomly chosen fields were observed under a fluorescence microscope (Leica, Wetzlar, Germany).

Statistical Analysis: All data were presented as the mean ± SEM and were analyzed by two-tailed Student's *t*-tests. *P* < 0.05 was considered significant, and *P* < 0.01 and *P* < 0.005 were highly significant.

Supporting Information

Supporting Information is available from the Wiley Online Library or from the author.

Acknowledgements

J.X. and H.W. contributed equally to this work. This work was supported by the National Natural Science Foundation of China (Grant Nos. 81501584, 81672651, 81502604, 81702973, 51873207, 51673190, 51603204, and 51673187), the Excellent Young Fund of Shanghai General Hospital (Grant No. 06N1702006), the Shanghai Municipal Health and Family Planning Commission (Grant No. 20164Y0270), and the Shanghai Hospital Development Center (Grant No. 16CR3010A).

Conflict of Interest

The authors declare no conflict of interest.

Keywords

autophagic degradation, autophagy, calcium/calmodulin-dependent protein kinase II α , fullerene C60 nanocrystals, osteosarcoma therapy

Received: July 30, 2018

Revised: December 4, 2018

Published online: February 10, 2019

- [1] X. Sun, X. Huang, J. Guo, W. Zhu, Y. Ding, G. Niu, A. Wang, D. O. Kiesewetter, Z. L. Wang, S. Sun, X. Chen, *J. Am. Chem. Soc.* **2014**, *136*, 1706.
- [2] R. Zhao, X. Han, Y. Li, H. Wang, T. Ji, Y. Zhao, G. Nie, *ACS Nano* **2017**, *11*, 8103.
- [3] S. Tong, C. A. Quinto, L. Zhang, P. Mohindra, G. Bao, *ACS Nano* **2017**, *11*, 6808.
- [4] A. Riedinger, T. Avellini, A. Curcio, M. Asti, Y. Xie, R. Tu, S. Marras, A. Lorenzoni, S. Rubagotti, M. Iori, P. C. Capponi, A. Versari, L. Manna, E. Seregini, T. Pellegrino, *J. Am. Chem. Soc.* **2015**, *137*, 15145.
- [5] S. P. Sherlock, S. M. Tabakman, L. Xie, H. Dai, *ACS Nano* **2011**, *5*, 1505.
- [6] H. W. Kroto, A. W. Allaf, S. P. Balm, *Chem. Rev.* **1991**, *91*, 1213.
- [7] Y. Liu, C. Chen, P. Qian, X. Lu, B. Sun, X. Zhang, L. Wang, X. Gao, H. Li, Z. Chen, J. Tang, W. Zhang, J. Dong, R. Bai, P. E. Lobie, Q. Wu, S. Liu, H. Zhang, F. Zhao, M. S. Wicha, T. Zhu, Y. Zhao, *Nat. Commun.* **2015**, *6*, 5988.
- [8] Y. Pan, L. Wang, S. G. Kang, Y. Lu, Z. Yang, T. Huynh, C. Chen, R. Zhou, M. Guo, Y. Zhao, *ACS Nano* **2015**, *9*, 6826.
- [9] Q. Li, L. Hong, H. Li, C. Liu, *Biosens. Bioelectron.* **2017**, *89*, 477.
- [10] H. Wang, P. Agarwal, S. Zhao, J. Yu, X. Lu, X. He, *Nat. Commun.* **2015**, *6*, 10081.
- [11] J. Shi, B. Wang, L. Wang, T. Lu, Y. Fu, H. Zhang, Z. Zhang, *J. Controlled Release* **2016**, *235*, 245.
- [12] Y. Miao, J. Xu, Y. Shen, L. Chen, Y. Bian, Y. Hu, W. Zhou, F. Zheng, N. Man, Y. Shen, Y. Zhang, M. Wang, L. Wen, *ACS Nano* **2014**, *8*, 6131.
- [13] L. Chen, Y. Miao, L. Chen, J. Xu, X. Wang, H. Zhao, Y. Shen, Y. Hu, Y. Bian, Y. Shen, J. Chen, Y. Zha, L. P. Wen, M. Wang, *Biomaterials* **2014**, *35*, 9269.
- [14] T. Wang, S. M. Guo, Z. Liu, L. C. Wu, M. C. Li, J. Yang, R. B. Chen, X. M. Liu, H. Xu, S. X. Cai, H. Chen, W. Y. Li, S. H. Xu, L. Wang, Z. Q. Hu, Q. Y. Zhuang, L. P. Wang, K. M. Wu, J. H. Liu, Z. Q. Ye, J. Y. Ji, C. G. Wang, K. Chen, *Oncotarget* **2014**, *5*, 10293.
- [15] C. Wang, N. Li, X. Liu, Y. Zheng, X. Cao, *J. Biol. Chem.* **2008**, *283*, 11565.
- [16] S. J. Chai, Y. Y. Qian, J. F. Tang, Z. Y. Liang, M. Zhang, J. X. Si, X. Z. Li, W. D. Huang, R. Z. Xu, K. Wang, *Cancer Lett.* **2014**, *344*, 119.
- [17] A. Britschgi, A. Bill, H. Brinkhaus, C. Rothwell, I. Clay, S. Duss, M. Rebhan, P. Raman, C. T. Guy, K. Wetzel, E. George, M. O. Popa, S. Lilley, H. Choudhury, M. Gosling, L. Wang, S. Fitzgerald, J. Borawski, J. Baffoe, M. Labow, L. A. Gaither, M. Bentires-Alj, *Proc. Natl. Acad. Sci. U. S. A.* **2013**, *110*, E1026.
- [18] M. D. Tzirakis, M. Orfanopoulos, *Chem. Rev.* **2013**, *113*, 5262.
- [19] H. Meng, G. Xing, B. Sun, F. Zhao, H. Lei, W. Li, Y. Song, Z. Chen, H. Yuan, X. Wang, J. Long, C. Chen, X. Liang, N. Zhang, Z. Chai, Y. Zhao, *ACS Nano* **2010**, *4*, 2773.
- [20] D. Yang, Y. Zhao, H. Guo, Y. Li, P. Tewary, G. Xing, W. Hou, J. J. Oppenheim, N. Zhang, *ACS Nano* **2010**, *4*, 1178.
- [21] Q. Zhang, W. Yang, N. Man, F. Zheng, Y. Shen, K. Sun, Y. Li, L. P. Wen, *Autophagy* **2009**, *5*, 1107.
- [22] K. H. Kim, M. S. Lee, *Nat. Rev. Endocrinol.* **2014**, *10*, 322.
- [23] G. Kroemer, B. Levine, *Nat. Rev. Mol. Cell Biol.* **2008**, *9*, 1004.
- [24] N. Mizushima, *Cell Death Differ.* **2005**, *12*, 12 Suppl 2, 1535.
- [25] S. T. Stern, P. P. Adisheshaiah, R. M. Crist, *Part. Fibre Toxicol.* **2012**, *9*, 20.
- [26] Y. Wang, X. Tai, L. Zhang, Y. Liu, H. Gao, J. Chen, K. Shi, Q. Zhang, Z. Zhang, Q. He, *J. Controlled Release* **2015**, *199*, 17.
- [27] P. Wei, L. Zhang, Y. Lu, N. Man, L. Wen, *Nanotechnology* **2010**, *21*, 495101.
- [28] M. S. Isakoff, S. S. Bielack, P. Meltzer, R. Gorlick, *J. Clin. Oncol.* **2015**, *33*, 3029.
- [29] K. Yuan, L. W. Chung, G. P. Siegal, M. Zayzafoon, *Lab. Invest.* **2007**, *87*, 938.
- [30] P. G. Daft, K. Yuan, J. M. Warram, M. J. Klein, G. P. Siegal, M. Zayzafoon, *Mol. Cancer Res.* **2013**, *11*, 349.
- [31] A. Hudmon, H. Schulman, *Annu. Rev. Biochem.* **2002**, *71*, 473.
- [32] P. Pellicena, H. Schulman, *Front. Pharmacol.* **2014**, *5*, 21.
- [33] B. Ravikumar, S. Sarkar, J. E. Davies, M. Futter, M. Garcia-Arencibia, Z. W. Green-Thompson, M. Jimenez-Sanchez, V. I. Korolchuk, M. Lichtenberg, S. Luo, D. C. Massey, F. M. Menzies, K. Moreau, U. Narayanan, M. Renna, F. H. Siddiqi, B. R. Underwood, A. R. Winslow, D. C. Rubinsztein, *Physiol. Rev.* **2010**, *90*, 1383.
- [34] N. Mizushima, T. Yoshimori, B. Levine, *Cell* **2010**, *140*, 313.
- [35] S. Pankiv, T. H. Clausen, T. Lamark, A. Brech, J. A. Bruun, H. Outzen, A. Overvatn, G. Bjorkoy, T. Johansen, *J. Biol. Chem.* **2007**, *282*, 24131.
- [36] X. Ma, Y. Wu, S. Jin, Y. Tian, X. Zhang, Y. Zhao, L. Yu, X. J. Liang, *ACS Nano* **2011**, *5*, 8629.

- [37] I. Schutz, T. Lopez-Hernandez, Q. Gao, D. Puchkov, S. Jabs, D. Nordmeyer, M. Schmutde, E. Ruhl, C. M. Graf, V. Haucke, *J. Biol. Chem.* **2016**, 291, 14170.
- [38] I. Funakoshi-Hirose, T. Aki, K. Unuma, T. Funakoshi, K. Noritake, K. Uemura, *Toxicology* **2013**, 312, 74.
- [39] A. V. Birk, E. J. Dubovi, L. Cohen-Gould, R. Donis, H. H. Szeto, *Virus Res.* **2008**, 132, 76.
- [40] E. J. Parkinson-Lawrence, T. Shandala, M. Prodoehl, R. Plew, G. N. Borlace, D. A. Brooks, *Physiology* **2010**, 25, 102.
- [41] F. Li, J. Wang, S. Sun, H. Wang, Z. Tang, G. Nie, *Small* **2015**, 11, 1954.
- [42] C. L. Vazquez, M. I. Colombo, *Methods Enzym.* **2009**, 452, 85.
- [43] H. Appelqvist, P. Waster, K. Kagedal, K. Ollinger, *J. Mol. Cell Biol.* **2013**, 5, 214.
- [44] Y. Y. Wang, R. Zhao, H. Zhe, *Oncotarget* **2015**, 6, 11725.
- [45] E. White, J. M. Mehnert, C. S. Chan, *Clin. Cancer Res.* **2015**, 21, 5037.
- [46] Z. Jing, X. Sui, J. Yao, J. Xie, L. Jiang, Y. Zhou, H. Pan, W. Han, *Cancer Lett.* **2016**, 372, 226.
- [47] P. Zhong, D. Quan, J. Peng, X. Xiong, Y. Liu, B. Kong, H. Huang, *J. Mol. Cell. Cardiol.* **2017**, 109, 1.
- [48] T. Cid-Diaz, I. Santos-Zas, J. Gonzalez-Sanchez, U. Gurriaran-Rodriguez, C. S. Mosteiro, X. Casabiell, T. Garcia-Caballero, V. Mouly, Y. Pazos, J. P. Camina, *J. Cachexia, Sarcopenia Muscle* **2017**, 8, 974.
- [49] C. Settembre, A. Fraldi, D. L. Medina, A. Ballabio, *Nat. Rev. Mol. Cell Biol.* **2013**, 14, 283.
- [50] X. Yu, Y. Long, H. Shen, *Autophagy* **2015**, 11, 1711.